Estimating the Observed Atmospheric Response to SST Anomalies: Maximum Covariance Analysis, Generalized Equilibrium Feedback Assessment, and Maximum Response Estimation

CLAUDE FRANKIGNOUL AND NADINE CHOUAIB

LOCEAN/IPSL, Université Pierre et Marie Curie, Paris, France

ZHENGYU LIU

Center for Climatic Research, University of Wisconsin—Madison, Madison, Wisconsin

(Manuscript received 26 February 2010, in final form 13 October 2010)

ABSTRACT

Three multivariate statistical methods to estimate the influence of SST or boundary forcing on the atmosphere are discussed. Lagged maximum covariance analysis (MCA) maximizes the covariance between the atmosphere and prior SST, thus favoring large responses and dominant SST patterns. However, it does not take into account the possible SST evolution during the time lag. To correctly represent the relation between forcing and response, a new SST correction is introduced. The singular value decomposition (SVD) of generalized equilibrium feedback assessment (GEFA–SVD) identifies in a truncated SST space the optimal SST patterns for forcing the atmosphere, independently of the SST amplitude; hence it may not detect a large response. A new method based on GEFA, named maximum response estimation (MRE), is devised to estimate the largest boundary-forced atmospheric signal. The methods are compared using synthetic data with known properties and observed North Atlantic monthly anomaly data. The synthetic data shows that the MCA is generally robust and essentially unbiased. GEFA–SVD is less robust and sensitive to the truncation. MRE is less sensitive to truncation and nearly as robust as MCA, providing the closest approximation to the largest true response to the sample SST. To analyze the observations, a 2-month delay in the atmospheric response is assumed based on recent studies. The delay strongly affects GEFA–SVD and MRE, and it is key to obtaining consistent results between MCA and MRE. The MCA and MRE confirm that the dominant atmospheric signal is the NAO-like response to North Atlantic horseshoe SST anomalies. When the atmosphere is considered in early winter, the response is strongest and MCA most powerful. With all months of the year, MRE provides the most significant results. GEFA–SVD yields SST patterns and NAO-like atmospheric responses that depend on lag and truncation, thus lacking robustness. When SST leads by 1 month, a significant mode is found by the three methods, but it primarily reflects, or is strongly affected by, atmosphere persistence.

1. Introduction

The climatic impact of anomalous extratropical sea surface temperature (SST) and other boundary forcing is difficult to detect as the natural variability of the atmosphere (which would occur in the absence of boundary forcing) is large outside the tropics, resulting in a small signal-to-noise ratio. At midlatitudes, the dominant large-scale air–sea interaction at interannual time scale reflects the stochastic atmospheric forcing of SST anomalies (Frankignoul and Hasselmann 1977). It largely determines the correlation between SST and the atmosphere when SST follows or is in phase, although the unlagged correlation between SST and surface heat flux is influenced by the atmospheric response (Frankignoul et al. 1998). The influence of the ocean (or other boundary forcing, hereafter referred to as SST forcing) must thus be estimated from the relation between SST anomalies and atmospheric fields lagging SST by more than the atmospheric persistence. Frankignoul et al. (1998) estimated the response of the surface heat flux to SST anomalies (termed heat flux feedback) from the ratio of the lagged covariance between SST and heat flux and

Corresponding author address: Claude Frankignoul, LOCEAN, Université Pierre et Marie Curie, 4 Place Jussieu, Paris, 75252 CEDEX, France.
E-mail: cf@locean-ipsl.upmc.fr

DOI: 10.1175/2010JCLI3696.1

© 2011 American Meteorological Society

the lagged SST autocovariance. The method has been used to estimate the local response to SST anomalies, land surface variability, and single SST patterns such as empirical orthogonal functions (EOF) (Frankignoul and Kestenare 2002; Liu and Wu 2004; Park et al. 2005; Z. Liu et al. 2006, 2007). However, it is not well adapted to the multivariate case when the forcing patterns are not specified a priori.

Hence, the large-scale atmospheric response to SST anomalies has been mostly derived with methods that determine the key SST patterns, such as lagged maximum covariance analysis (MCA) based on singlular value decomposition (SVD) (Czaja and Frankignoul 1999, 2002, hereafter referred to as CF99 and CF02, respectively; Rodwell and Folland 2002; Q. Liu et al. 2006; Frankignoul and Sennéchael 2007) or canonical correlation analysis (Friederichs and Hense 2003). The MCA determines the atmospheric and oceanic patterns that maximize the covariance between the two fields. It is a powerful method to investigate dominant ocean–atmosphere interactions since it favors large SST forcing and/or atmospheric response. In many previous applications, the most significant response was found when SST leads by several months, resulting in uncertainties in the SST amplitude since the SST may have evolved during the time lag (CF02), but consistent with modeling studies indicating that the atmospheric response only reaches its maximum amplitude after a few months owing to the time taken by transient eddies to fully alter the initial baroclinic response (Ferreira and Frankignoul 2005, 2008; Deser et al. 2007).

Another way to estimate the atmospheric response to SST forcing was introduced by Liu et al. (2008), who generalized the method of Frankignoul et al. (1998) to the multivariate case with the generalized equilibrium feedback assessment (GEFA). As GEFA involves inverting the lagged covariance matrix of the SST anomalies, it is sensitive to sampling errors and spatial resolution of the SST anomalies and is thus used in truncated SST EOF space. GEFA can be combined with SVD to extract optimal coupled modes, which describe the atmospheric patterns that are most sensitive to SST anomaly forcing (Liu and Wen 2008, hereafter referred to as LW08). However, GEFA–SVD will not give large signals if the optimal SST anomalies are small. As large signals are of most interest in climate studies, we devise a new method based on GEFA, named maximum response estimation (MRE), which directly estimates the largest SST-forced atmospheric modes.

The aim of this study is to compare the three methods and assess their biases and robustness. With a climate application in mind, we also discuss which method is better to estimate the strongest atmospheric response. The methods are described in section 2, where we show how to take into account the SST anomaly evolution in the lagged MCA to correctly represent the relation between forcing and response. In section 3, the three methods are applied to synthetic data with known properties. In section 4, the methods are used to detect North Atlantic SST anomaly influence in the observations.

2. The three multivariate methods

Let $\mathbf{X}$ denote the atmospheric data matrix, with J points and L time bins, and $\mathbf{T}$ the SST matrix, with I points and L time bins. Assuming instantaneous linear atmospheric response, one has

$$\mathbf{X}(t) = \mathbf{F}\mathbf{T}(t) + \mathbf{N}(t), \tag{1}$$

where $\mathbf{F}$ is the feedback matrix, and $\mathbf{N}(t)$ represents stochastic forcing by the atmospheric intrinsic variability, which is independent of $\mathbf{T}(t)$. Other persistent atmospheric components such as being due to ENSO teleconnections are assumed to be negligible or to have been removed.

The covariance matrix between $\mathbf{X}$ and $\mathbf{T}$ at lag τ is estimated by

$$\mathbf{C}_{\mathbf{XT}}(\tau) = \frac{1}{L}\sum_{t} \mathbf{X}(t)\mathbf{T}^{\mathrm{T}}(t-\tau), \tag{2}$$

where the superscript T denotes transpose. For negative τ (atmosphere leads) and, in most cases, $\tau = 0$, $\mathbf{C}_{\mathbf{XT}}(\tau)$ primarily reflects the oceanic response to the atmospheric forcing. For positive τ larger than the intrinsic atmospheric persistence, $\mathbf{C}_{\mathbf{XT}}(\tau)$ reflects the atmospheric response to the boundary forcing. Indeed, introducing (1) in (2) with $\mathbf{C}_{\mathbf{XT}}(\tau) = 0$ yields

$$\mathbf{C}_{\mathbf{XT}}(\tau) = \frac{1}{L}\sum_{t} \mathbf{F}\mathbf{T}(t)\mathbf{T}^{\mathrm{T}}(t-\tau) = \mathbf{F}\mathbf{C}_{\mathbf{TT}}(\tau), \tag{3}$$

which only depends on $\mathbf{F}$ and $\mathbf{T}$. The e-folding time scale of large-scale atmospheric patterns such as the North Atlantic Oscillation (NAO) does not exceed 10 days (Feldstein 2000), hence a lag ≥ 1 month has often been used to single out the atmospheric response with monthly averaged data. However, we argue below that $\mathbf{C}_{\mathbf{XT}}(\tau)$ is still affected by atmospheric persistence at a lag of 1 month, so that a larger lag should be used.

a. Lagged MCA

To estimate the atmospheric response to SST, the MCA (e.g., Bretherton et al. 1992; von Storch and Zwiers 1999) determines the atmospheric and oceanic patterns

that maximize the covariance at (positive) lag τ between $\mathbf{X}$ and $\mathbf{T}$ by decomposing them into

$$\mathbf{X}(t) = \sum_{1}^{K} \mathbf{u}_k a_k(t) = \mathbf{U}\mathbf{A}^{\mathrm{T}}(t) \quad \text{and} \tag{4}$$

$$\mathbf{T}(t-\tau) = \sum_{1}^{K} \mathbf{v}_k b_k(t-\tau) = \mathbf{V}\mathbf{B}^{\mathrm{T}}(t-\tau), \tag{5}$$

where the $\mathbf{u}$ and $\mathbf{v}$ are the K orthonormal left and right singular vectors of $\mathbf{C}_{\mathbf{XT}}(\tau)$. The SVD of the covariance matrix is

$$\mathbf{C}_{\mathbf{XT}}(\tau) = \frac{1}{L}\mathbf{U}\mathbf{A}^{\mathrm{T}}(t)\mathbf{B}(t-\tau)\mathbf{V}^{\mathrm{T}} = \mathbf{U}\mathbf{D}\mathbf{V}^{\mathrm{T}}, \tag{6}$$

where $\mathbf{D}$ is the diagonal matrix of the singular values $\boldsymbol{\sigma}_k$, decreasing for increasing k. The first singular value defines the atmospheric and oceanic patterns that have the largest lagged covariance. The (dimensional) time series are given by

$$a_j(t) = \mathbf{u}_j^{\mathrm{T}}\mathbf{X}(t), \quad b_j(t-\tau) = \mathbf{v}_j^{\mathrm{T}}\mathbf{T}(t-\tau). \tag{7}$$

To describe the patterns, it is convenient to show the so-called homogeneous covariance map of $\mathbf{T}$ and the heterogeneous covariance map of $\mathbf{X}$, given by the regression of $\mathbf{T}(t-\tau)$ and $\mathbf{X}(t)$ onto the SST time series $b_j(t-\tau)$, respectively, which preserve linear relations between the variables (CF02). We show scaled homogeneous and heterogeneous covariance maps that represent the atmospheric response (say in m) to the SST anomaly (in K) τ month earlier whose time series is the normalized value of $b_j(t-\tau)$ (see appendix).

These relations are appropriate for predictive purposes as they maximize the covariance between SST and the atmosphere at a later time, but they do not represent an equilibrium response solution as they do not take into account the SST change during time τ. To derive the equilibrium atmospheric response, we multiply (3) by $\boldsymbol{\nu}_k$ and use (6), yielding

$$\boldsymbol{\sigma}_k\mathbf{u}_k = \mathbf{F}\mathbf{C}_{\mathbf{TT}}(\tau)\mathbf{v}_k = \mathbf{F}\mathbf{q}_k. \tag{8}$$

Based on (1), the equilibrium atmospheric response to the SST forcing $\mathbf{q}_k = \mathbf{C}_{\mathbf{TT}}(\tau)\mathbf{v}_k$ is $\boldsymbol{\sigma}_k\mathbf{u}_k$. The comparison with the homogeneous covariance map (A1) shows that $\boldsymbol{\nu}_k$ is multiplied by $\mathbf{C}_{\mathbf{TT}}(\tau)$ instead of $\mathbf{C}_{\mathbf{TT}}(0)$. This gives a larger atmospheric sensibility since the SST is reduced but the atmospheric signal unchanged. However, autocovariance estimates are negatively biased, especially at large lag and when the true autocorrelation is large (von Storch and Zwiers 1999), so that the SST correction may overestimate the atmospheric sensitivity. Scaled corrected homogeneous and heterogeneous covariance maps are obtained by normalizing the time series describing the evolution of $\mathbf{q}_k$ (see appendix). To interpret (8), we may consider an autoregressive model for the SST, given at a time lead τ from an initial SST pattern $\mathbf{T}(t)$ by

$$\mathbf{T}(t+\tau) = \mathbf{A}\mathbf{T}(t) + \boldsymbol{\varepsilon}, \tag{9}$$

where $\boldsymbol{\varepsilon}$ is random noise. The optimal prediction is made with the propagator $\mathbf{A}$

$$\mathbf{A} = \mathbf{C}_{\mathbf{TT}}(\tau)\mathbf{C}_{\mathbf{TT}}(0)^{-1}. \tag{10}$$

If $\mathbf{T}(t)$ is the uncorrected SST homogeneous covariance map (A1), the predicted SST is

$$\mathbf{A}\mathbf{T}(t) = \mathbf{C}_{\mathbf{TT}}(\tau)\mathbf{C}_{\mathbf{TT}}(0)^{-1}\mathbf{C}_{\mathbf{TT}}(0)\mathbf{v}_k = \mathbf{C}_{\mathbf{TT}}(\tau)\mathbf{v}_k = \mathbf{q}_k. \tag{11}$$

The corrected SST pattern $\mathbf{q}_k$ can thus be thought of as the time evolution of the original pattern of uncorrected SST after a time τ.

Statistical significance of the MCA modes can be tested using a moving block bootstrap approach, linking the original SST anomalies with randomly scrambled atmospheric ones, and comparing the square covariance, correlation, and square covariance fraction with the randomized ones (CF02; Rodwell and Folland 2002).

b. GEFA

The GEFA method of Liu et al. (2008) estimates the feedback matrix $\mathbf{F}$ from (3)

$$\mathbf{F} = \mathbf{C}_{\mathbf{XT}}(\tau)\mathbf{C}_{\mathbf{TT}}(\tau)^{-1}. \tag{12}$$

This requires inverting the SST covariance matrix. As the historical record is limited, sampling error can be large, in particular at large lag, and a regularization method is needed. The inversion is done in a truncated EOF space. However, it requires choosing the optimal EOF truncation, a difficult issue (Liu et al. 2008; LW08). GEFA can be used to estimate the atmospheric response to prescribed SST patterns, such as SST EOFs (Wen et al. 2010).

GEFA can also be used to estimate optimal feedback modes by performing a SVD of the feedback matrix (LW08). If the SVD decomposition of $\mathbf{F}$ is the $\mathbf{L}$ (left) and $\mathbf{R}$ (right) orthogonal fields, with SVD values $\boldsymbol{\gamma}_j$, we have

$$\mathbf{C_{TX}}(\tau)\mathbf{C_{TT}}(\tau)^{-1} = \mathbf{F} = \mathbf{LSR}^{\mathrm{T}} = \sum \boldsymbol{\gamma}_j \mathbf{l}_j \mathbf{r}_j^{\mathrm{T}}. \quad (13)$$

Right multiplication by $\mathbf{r}_k$ yields

$$\boldsymbol{\gamma}_k \mathbf{l}_k = \mathbf{F}\mathbf{r}_k, \quad (14)$$

so that $\mathbf{r}_1$ is the optimal SST forcing pattern that forces an atmospheric response pattern $\boldsymbol{l}_1$ with a magnitude $\boldsymbol{\gamma}_1$. It is, however, sensitive to EOF truncation (LW08, see also below). The dimensional form is obtained as in (A4).

The optimal mode describes the pair of patterns that reflects the largest atmospheric sensitivity to SST anomalies. The optimization in GEFA pertains to the feedback matrix. Hence, it identifies the SST pattern that produces the strongest possible atmospheric response among all possible SST patterns of the same magnitude. If the sample SST variability is not dominated by this optimal SST pattern, the atmospheric signal may be small. Statistical significance is tested as for the MCA by comparing the singular values of **F** to randomized ones.

c. MRE

Since GEFA–SVD may not detect a large atmospheric signal, we introduce the MRE method that aims at detecting the largest boundary forced atmospheric signals. It seeks to maximize the magnitude of the atmospheric response in a given dataset. Since the signal is given from (1) by $\mathbf{FT}(t)$, the largest response is obtained by calculating the main EOFs of $\mathbf{FT}(t)$, which maximize the represented variance. If **F** is known, the calculation is straightforward. Otherwise, **F** can be estimated as in GEFA in a truncated SST space. The EOFs of **FT** are the eigenvectors of the covariance matrix

$$\begin{aligned}\mathbf{C_{FT\,FT}}(0) &= \mathbf{F}\mathbf{C_{TT}}(0)\mathbf{F}^{\mathrm{T}} \\ &= \mathbf{C_{TX}}(\tau)\mathbf{C_{TT}}(\tau)^{-1}\mathbf{C_{TT}}(0)\mathbf{C_{TT}}(\tau)^{-1}\mathbf{C_{TX}}(\tau)^{\mathrm{T}},\end{aligned} \quad (15)$$

providing orthogonal estimates of the largest atmospheric response patterns $\mathbf{p}_i$

$$\mathbf{FT}(t) = \sum_i c_i(t)\mathbf{p}_i. \quad (16)$$

The SST anomalies that generated the response are found by regressing the original SST anomaly field $\mathbf{T}(t)$ onto the principal components $c_i(t)$ and dimensional patterns obtained by normalizing the latter. Although the MRE also involves estimating **F** and thus inverting the SST covariance matrix, it is shown below to be more robust and less sensitive to the EOF truncation than GEFA–SVD. This presumably occurs because the dominant SST anomalies tend to have a large scale, which filters out the sampling errors of **F** in (16). Statistical significance is tested by scrambling the atmospheric time sequence to build the distribution of the randomized eigenvalues of **FT** under the null hypothesis of no true signal.

d. Delayed atmospheric response

Model response to fixed or interactive SST anomalies (Ferreira and Frankignoul 2005, 2008; Deser et al. 2007) and statistical analysis (Strong et al. 2009) suggests that the large-scale atmospheric response to persistent boundary forcing only reaches its maximum amplitude after a few months.[1] This might explain why the covariance and the statistical significance were stronger in the MCA when the atmosphere lagged SST by 3 or 4 months than by 1 or 2 months in CF02 and Frankignoul and Sennéchael (2007). If the atmospheric response takes weeks or months to reach its maximum amplitude, $\mathbf{FT}(t)$ in (1) should be replaced by $\int_0^t \mathbf{F}(u)\mathbf{T}(u)\,du$. A response that depends on a weighted integral of the SST evolution could be modeled by a time-delay vector, but estimating it would increase the dimensionality and the complexity of the analysis. However, the transient atmospheric response in the model studies above approximately obeys

$$\frac{dX}{dt} = -\frac{X}{\alpha} + \beta T(t), \quad (17)$$

where α defines the response time and β the amplitude. For $t \gg \alpha$, the solution is

$$\begin{aligned}X(t) &= \beta \int_0^t T(u)\exp\left(-\frac{t-u}{\alpha}\right) du \\ &= \alpha\beta T(t^*)\left[1 - \exp\left(-\frac{t}{\alpha}\right)\right] \approx \alpha\beta T(t^*)\end{aligned} \quad (18)$$

if we use the mean value theorem. Hence, relation (1) can be replaced by

$$\mathbf{X}(t) = \mathbf{FT}(t-a) + \mathbf{N}(t), \quad (19)$$

where the delay $a = t - t^*$ is likely to be rather close to α. The MCA correction in (8) should then be based on $\mathbf{C_{TT}}(\tau - a)$ rather than $\mathbf{C_{TT}}(\tau)$ for $\tau \geq a$. For $0 \leq \tau < a$, we use $\mathbf{C_{TT}}(0)$, lacking a better model. In GEFA and MRE, (12) should be similarly replaced by

$$\mathbf{F} = \mathbf{C_{XT}}(\tau)\mathbf{C_{TT}}(\tau - a)^{-1}, \quad (20)$$

[1] This does not hold for the atmospheric boundary layer, which responds rapidly.

which decreases the sensitivity of $\mathbf{F}$ to sampling errors since the SST covariance matrix is estimated at shorter lag. In MRE, the SST patterns that generated the largest responses are obtained by regressing $\mathbf{T}(t - a)$ onto the EOF time series.

Note that the atmospheric response time to SST forcing is larger than the *e*-folding time scale of large-scale atmospheric patterns as it results from different physics. The former reflects the time it takes for the transient eddies to alter the initial baroclinic atmospheric response into a full-grown equivalent barotropic one (Ferreira and Frankignoul 2005; Deser et al. 2007). The latter is determined by internal atmospheric dynamics.

3. Application to a simple advective stochastic climate model

a. The model

To compare the methods, we use the conceptual stochastic climate model of Liu et al. (2008) that includes nonlocal atmospheric advection. The coupled model, in nondimensional form in the domain $0 \le x \le 1$, consists of the atmospheric equation

$$\partial T_a/\partial x = \lambda(T - T_a) + n(x,t) \tag{21}$$

and the oceanic equation

$$\partial T/\partial t = H - dT, \tag{22}$$

where T_a is air temperature, T is SST, $H = T_a - T$ is the downward heat flux, and d is the oceanic damping. The relative importance of local coupling versus nonlocal advection is measured by λ, a smaller λ representing a stronger advection or, equivalently, a weaker local coupling. The atmospheric response to a SST anomaly $T(x, t)$ is instantaneous and can be obtained by integrating the equilibrium atmospheric Eq. (21) downwind along x. After digitizing into I spatial intervals, the atmospheric response can be put in the form (1) (see Liu et al. 2008 for more details), where $\mathbf{X}$ represents the air temperature and $\mathbf{N}$ a transformed stochastic forcing given by $\mathbf{N}(t) = (\mathbf{B}/\boldsymbol{\lambda})n(t) + q_b$. Here, the air temperature at the upstream boundary $x = 0$ is $\mathbf{T}_{a0}(t)$, which decays downwind following $\mathbf{q}_b^{\mathrm{T}} = (q, q^2 \ldots q^I)$ with $q = e^{-\lambda\Delta x} < 1$. The feedback matrix, given by

$$\mathbf{F} = \lambda\Delta x \begin{bmatrix} 1 & 0 & .. & 0 \\ q & 1 & .. & 0 \\ .. & .. & .. & .. \\ q^{I-1} & q^{I-2} & .. & 1 \end{bmatrix} \tag{23}$$

can be interpreted as follows. The positive diagonal elements represent the local air temperature response to SST. The positive off-diagonal elements represent the nonlocal response, with the ith row representing the response T_{ai} to all the upstream SSTs $T_j (j \le i)$, whose influence decays downwind with the distance following an increasing power of q. Alternatively, the jth column represents the remote impacts of T_j on all downstream air temperature T_{ai} $(i \ge j)$, which also decay downwind with the distance. The coupled system in terms of SST is obtained by inserting (1) into (22) as

$$d\mathbf{T}/dt = (\mathbf{F} - \mathbf{I})\mathbf{T}(t) + \mathbf{N}(t) - d\mathbf{T}, \tag{24}$$

where $\lambda\Delta x < 1$ is required for the Courant–Friedrichs–Lewy (CFL) numerical stability criterion.

As in LW08, we consider a 12-point model that is forced by independent stochastic forcing in the interior and at the upstream boundary. The forcing is either spatially uncorrelated (12 spatial degrees of freedom, hereafter df) or a dipole with identical stochastic forcing in the first and the last 6 points (2 df). A sample size of $L = 800$ is used for each realization, with the data binned in a time interval of 0.5. A 500-member ensemble is performed in each case. We will discuss a weak advection case ($\lambda = 4.8$, $d = 0$) and a strong advection case ($\lambda = 1.2$, $d = 0$), focusing on the first two modes and lag ≤ 5. The figures below show for each mode the mean SST (the average SST pattern of the mode over the 500 realizations), the true mean atmospheric response obtained by applying the true $\mathbf{F}$ to the mean SST, and the mean atmospheric response based on the estimated $\mathbf{F}$ in each of the 500 realizations. What quantifies the robustness of the method is the uncertainty of the estimated atmospheric response, given for each mode by the 95% confidence interval derived at each grid point from the distribution of the difference between estimated and true response to the SST in each of the 500 realizations. The results are robust when the estimated response has a small uncertainty, hence is systematically close to the true one, but not when the scatter is large (large uncertainty). The response will be considered as "well determined" if it is significantly different from zero at more than half of the 12 grid points, a subjective but conservative choice (see section 3e).

b. Lagged MCA

In the most idealized case (weak advection, 12 df), the estimated atmospheric response is unbiased and its uncertainty very small, so we show the modes at lag 5 (Fig. 1, left). The MCA takes into account the SST amplitude, thus favoring dominant SST patterns. In the present case, the SST variability increases downstream, hence

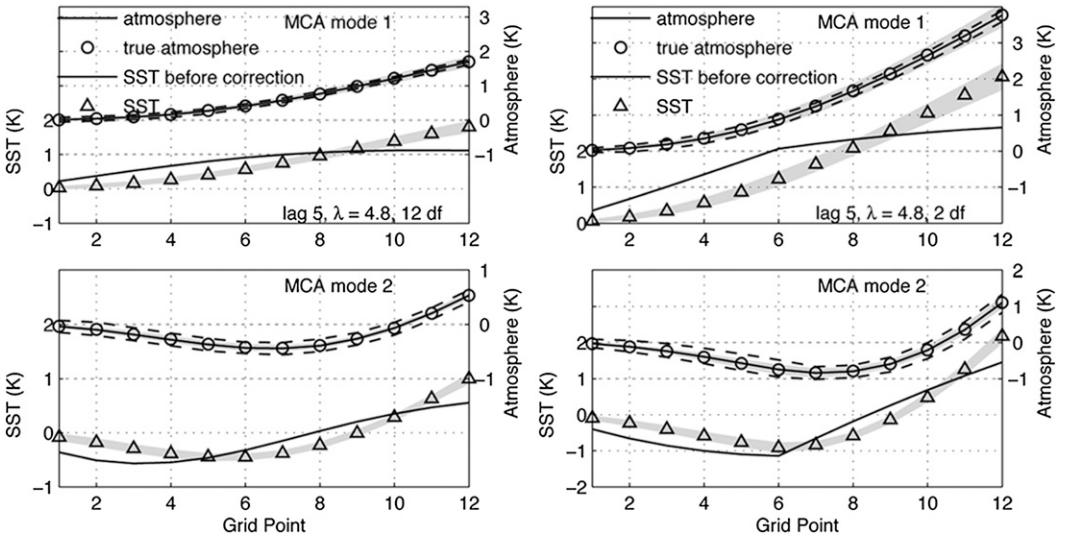

FIG. 1. MCA mode (top) 1 and (bottom) 2 at lag 5 in the weak advection case with (left) spatially uncorrelated (12 df) and (right) correlated (2 df) forcing. The mean SST is given by triangles, the mean estimated atmospheric response by the upper continuous line, the true response to the mean SST by circles, and the mean SST before correction by the lower continuous line. Gray shading corresponds to ±1 standard deviation and the dashed line indicates the uncertainty (see text). Units are in K.

the SST in the first MCA mode also increases downstream. The uncertainty is even smaller at shorter lag, and the patterns are similar, but for a slight upstream shift, as expected from the atmospheric advection. Using correlated atmospheric forcing (2 df) only slightly increases the uncertainty (Fig. 1, right). In both cases, the SST correction (8) is crucial to representing the forcing pattern as the SST before correction (lower continuous lines) is somewhat different, especially at large lag. Omitting the SST correction, as in previous applications of the MCA, leads to a biased relation between forcing and response.

As in LW08, the strong advection case proves more difficult and only mode 1 is well determined. The uncertainty becomes large by lag 4, hence we show the results for lag 2, the largest lag yielding a reasonably well-determined response for both uncorrelated (Fig. 2, top) and correlated (bottom) forcing. Again, the lagged MCA is basically unbiased.

c. *GEFA–SVD*

The calculation was made in truncated EOF space using the first 3, 5, and 7 EOFs (hereafter TR3, TR5, and TR7). In the weak advection case with uncorrelated forcing, the first two GEFA–SVD modes are nearly unbiased at lag 1 and 2, but the uncertainty is larger than in the MCA, and it increases with the number of EOFs. As discussed by Liu et al. (2008), GEFA deteriorates at large lag and depends sensitively on the EOF truncation because of decreasing SST autocovariance, sampling errors, and increasing covariance among different SST PCs. We show in Fig. 3 (left) the two modes in TR5 at lag 2, the largest lag for which they are both well determined (mode 1 remains well determined until lag 5 in TR3, lag 3 in TR5, and lag 2 in TR7). The patterns strongly differ from those of the MCA and the amplitude is smaller,

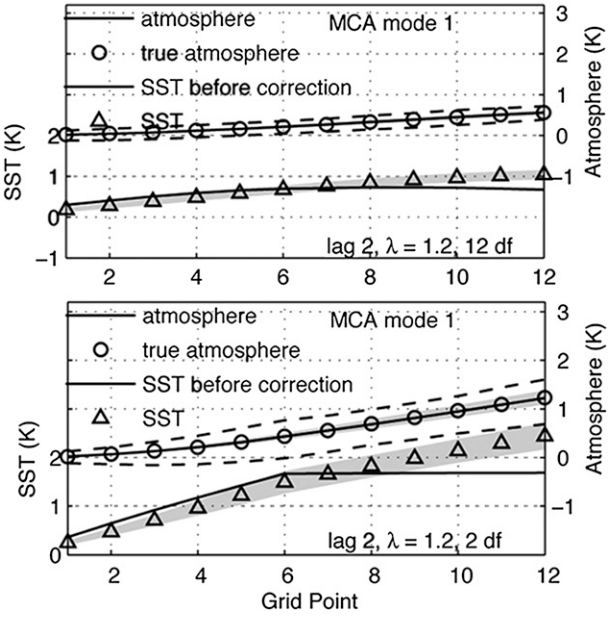

FIG. 2. As in Fig. 1, but for mode 1 at lag 2 in the strong advection case with (top) uncorrelated and (bottom) correlated forcing.

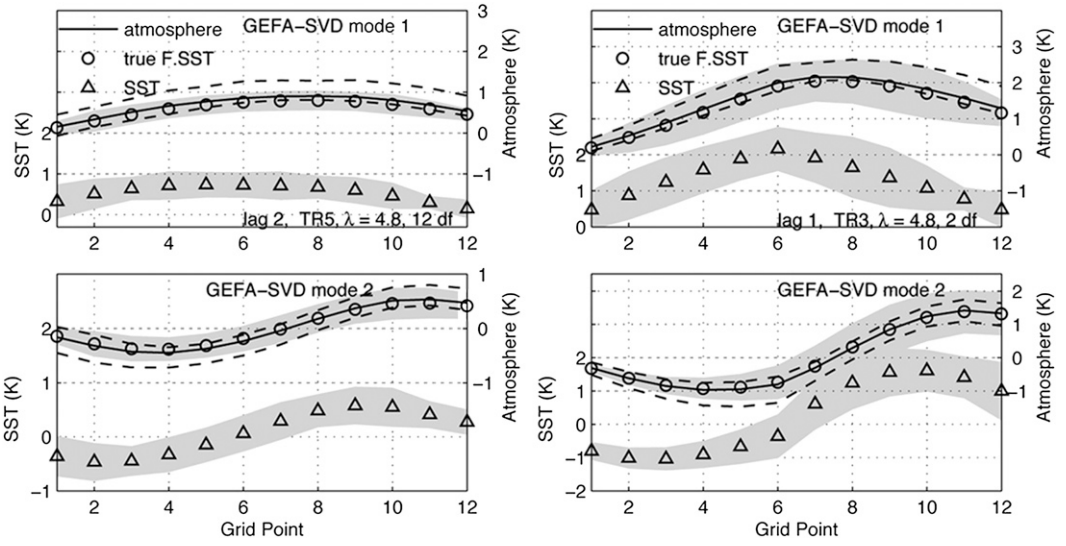

FIG. 3. GEFA–SVD mode (top) 1 and (bottom) 2 in the weak advection case at (left) lag 2 in TR5 with spatially uncorrelated forcing and (right) lag 1 in TR3 with correlated forcing, showing the mean SST (triangle), the mean estimated atmospheric response (continuous line), and the true response to the mean SST (circle). The gray shading corresponds to ±1 standard deviation, and the dashed line indicates the uncertainty. Units are in K.

reflecting that GEFA–SVD maximizes the atmospheric sensitivity independently from the SST amplitude.

In more difficult cases, GEFA–SVD may only provide well determined, albeit slightly biased, modes at lag 1 and in TR3, a strongly truncated EOF space. The two modes are (moderately) well determined in the weak advection case with correlated forcing but with a large dispersion of the 500-member ensemble (Fig. 3, right). For strong advection, only mode 1 can be reliably estimated and solely for uncorrelated forcing (Fig. 4). Hence, GEFA–SVD only provides reliable estimates in favorable cases. It depends sensitively on the EOF truncation, as discussed by LW08, who suggested empirical rules to determine the optimal truncation.

d. MRE

The MRE proves to be more robust than GEFA–SVD and less sensitive to lag and EOF truncation. In the weak advection case with uncorrelated forcing, the first two modes are well-determined, unbiased estimates of the maximum atmospheric responses as derived from the true **F** until lag 4 or 5, depending on truncation (lag 5 in TR3, lag 4 in TR5 and TR7). As illustrated in Fig. 5 (left), the modes broadly resemble those obtained with MCA, reflecting that MCA favors large signals. For correlated forcing, the results remain very good at small lag; however, at large lag, a strong truncation is needed, as both modes only remain well determined and nearly unbiased until lag 4 in TR3, lag 3 in TR5 (Fig. 5, right), and lag 2 in TR7.

As with the other methods, only the first mode can be confidently estimated in the large advection case. MRE is nearly as robust as MCA since, for uncorrelated (correlated) forcing, it remains well determined until lag 2 (lag 2) in TR3, lag 2 (lag 1) in TR5 (Fig. 6), and lag 1 (lag 1) in TR7. However, the atmospheric response is biased high in Fig. 6, although the bias is very small at smaller truncation or shorter lag, as in Fig. 7 below.

e. Summary

The mean atmospheric response patterns are compared for the first two modes in Fig. 7 for weak (top) and strong (bottom) advection with uncorrelated forcing. The SST patterns were shown above, and all estimates are based on lag 1. For GEFA–SVD and MRE, we use TR5, except in the strong advection case where GEFA–SVD

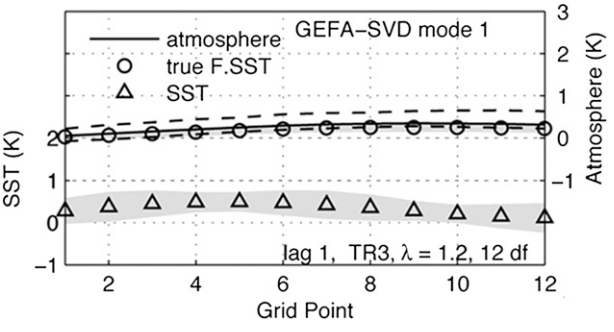

FIG. 4. As in Fig. 3, but for the first GEFA–SVD mode in the strong advection case at lag 1 in TR3 with uncorrelated forcing.

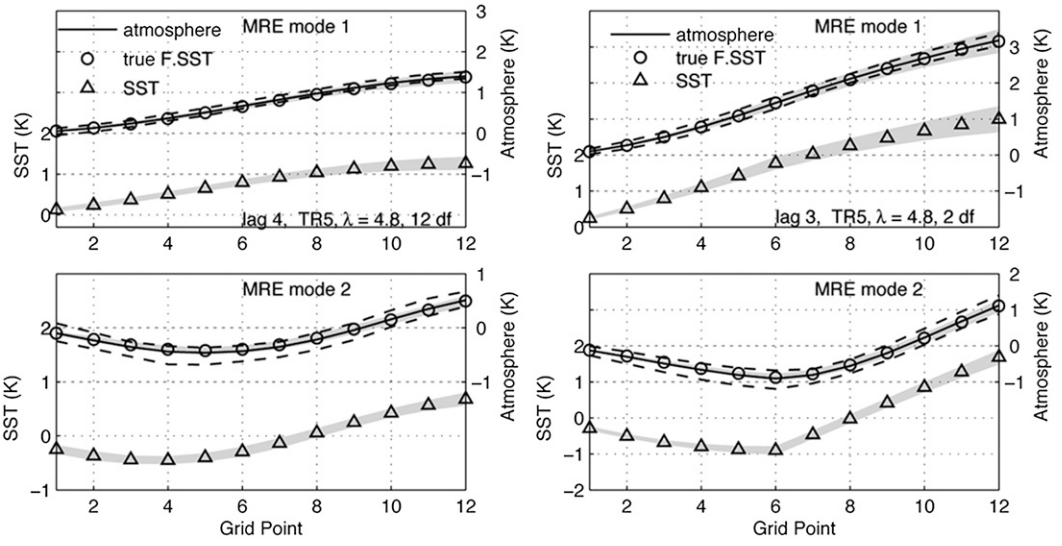

FIG. 5. MRE mode (top) 1 and (bottom) 2 in TR5 in the weak advection case with (left) spatially uncorrelated and (right) correlated forcing at lags 4 and 3, respectively. The mean SST is given by triangles, the mean estimated atmospheric response by the continuous line, and the true response to the mean SST by circles. Gray shading corresponds to ±1 standard deviation and the dashed line the uncertainty. Units are in K.

is in TR3. For completeness, we also show the atmospheric response obtained by applying GEFA to the first two SST EOFs (hereafter GEFA–EOF), as in Wen et al. (2010).

For weak advection (top), MRE provides for both modes unbiased estimates of the largest atmospheric responses, and this holds for correlated forcing. The lagged MCA gives atmospheric modes that are pretty similar to the true largest ones but slightly smaller for mode 1 and shifted downstream. The atmospheric response obtained with GEFA–EOF1 resembles the first MCA mode. However, the response to GEFA–EOF2 differs. As expected from the different maximization criterion, the atmospheric signals estimated by GEFA–SVD are different and smaller for mode 1. At larger lag (not shown), the comparison is similar and MRE keeps providing unbiased estimators of the largest true responses. Mode 1 in the lagged MCA underestimates a little more the maximum true responses with increasing lag, while GEFA–EOF1 remains a good estimator of the largest true response. On the other hand, the GEFA–SVD modes only remain stable until lag 2 and, to a lesser extent, lag 3.

In the strong advection case (Fig. 7, bottom left), the first MRE mode at lag 1 is most similar to the largest true response, albeit slightly overestimated (but not in TR3). The response given by MCA is broadly similar but slightly smaller and shifted downstream, while GEFA–EOF1 is closer to the largest true response. The atmospheric signal in GEFA–SVD is different and weaker. As the lag increases, it is found that in TR5 (but not in TR3), MRE substantially overestimates the response (Fig. 6) and becomes useless by lag 3 or 4. GEFA–EOF also degrades at large lag, but the MCA mode remains very stable. Similar behaviors are found for correlated forcing, where the only method whose bias does not increase with increasing

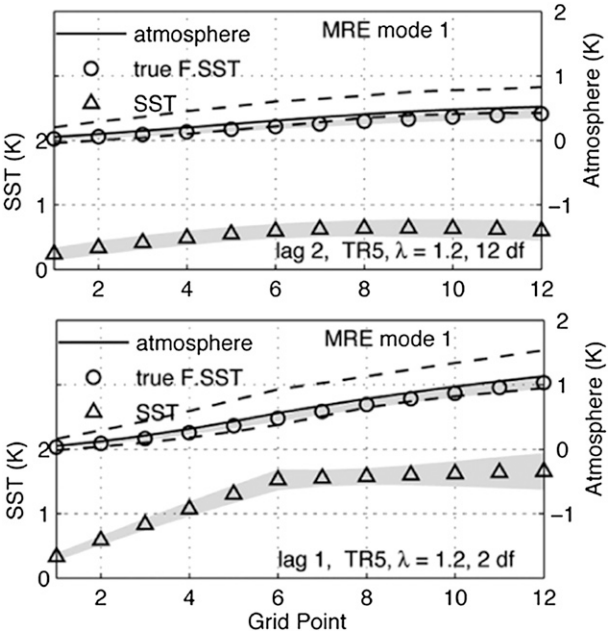

FIG. 6. As in Fig. 5, but in the strong advection case at (top) lag 2 with uncorrelated forcing and (bottom) lag 1 with correlated forcing.

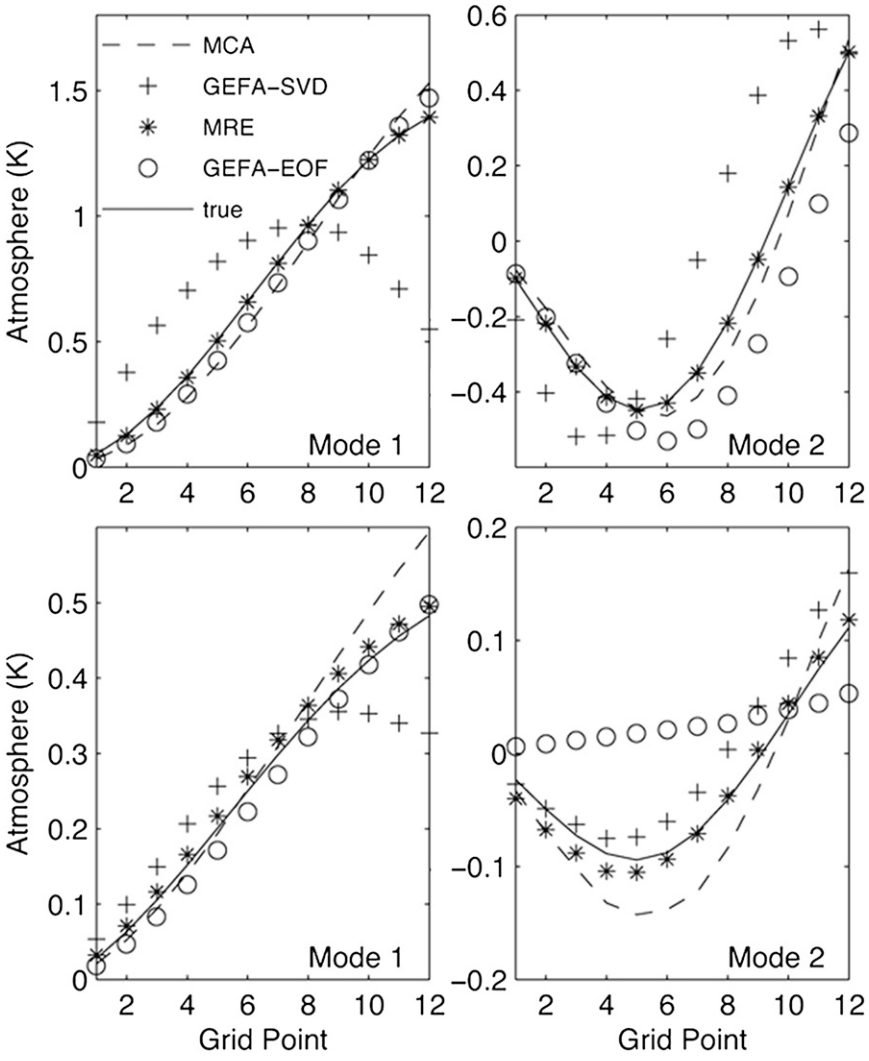

FIG. 7. Comparison between the (left) first and (right) second atmospheric response mode in the (top) weak and (bottom) strong advection case estimated at lag 1 with the lagged MCA (dashed), GEFA–SVD (crosses), MRE (stars), and GEFA–EOF (circles). The last three methods are based on TR5, except for GEFA–SVD in the strong advection case, based on TR3. The maximum true response is shown in continuous line. All amplitudes are given for normalized SST time series.

lag is MCA. Since one does not know in a practical application if the atmospheric response is well determined, we also show the poorly determined mode 2 (Fig. 7, bottom right). MRE and MCA are close to the second true largest response. This holds until lag 3, suggesting that our definition of ''well determined'' in section 3a may be too strict. On the other hand, GEFA–SVD and GEFA–EOF show little stability as the signal changes with the lag.

In summary, the stochastic model suggests that MRE is the most accurate method if one seeks the oceanic influence that explains most atmospheric variance, although it fails at large lag in unfavorable cases. The MCA provides slightly smaller but more robust estimates of the largest atmospheric response. GEFA–SVD is less robust and detects a different, smaller signal. GEFA–EOF also provides a good estimate of the largest atmospheric response for SST EOF1 but not SST EOF2, so that GEFA–EOF may not always identify large responses.

4. Application to observed air–sea interactions in the North Atlantic

To compare MCA, GEFA–SVD, and MRE in a realistic setting, we consider monthly anomaly data in the

North Atlantic sector where previous studies based on lagged MCA (CF99, CF02; Frankignoul and Kestenare 2005) found that a NAO-like signal during early winter was significantly linked to a prior horseshoe SST anomaly pattern (hereafter NAH). However, different modes were found in year-round data using GEFA–SVD (LW08) and GEFA–EOF (Wen et al. 2010). We focus on the relation between prior SST anomalies and geopotential height anomalies at 500 hPa (hereafter Z500) in the North Atlantic sector (10°–70°N, 100°W–20°E), using the National Centers for Environmental Prediction (NCEP)–National Center for Atmospheric Research (NCAR) reanalysis for 1958–2008 (Kistler et al. 2001), area weighting, and either monthly anomalies for the whole year, which provides the largest sample but may mix different atmospheric dynamics, or atmospheric anomalies in November–January (hereafter NDJ), when the signal was most significant in CF02. We consider SST in a large (10°–70°N, 100°W–10°E) and a small (20°–60°N, 80°W–0°) domain to investigate the robustness of the methods. A cubic trend was removed from all data to reduce the influence of trends and ultralow frequencies. The ENSO signal was removed by regression onto the first two principal components of tropical Pacific SST anomalies, taking into account the phase asymmetry of ENSO teleconnections, as in Frankignoul and Kestenare (2005). Statistical significance was estimated using a bootstrap approach with 500 randomized atmospheric sequences. We only discuss the first mode since higher modes were generally not significant or robust. Only significant modes at the 10% level are shown.

As discussed in section 2d, the large-scale atmospheric response to extratropical SST anomalies cannot be considered as instantaneous on the monthly time scale. This was represented by introducing the delay a in (18). We used $a = 2$ months. The lagged MCA is not very sensitive to the choice of a since it affects the SST anomaly pattern and the amplitude of the atmospheric response but not the atmospheric pattern nor its statistical significance. On the other hand, GEFA–SVD and MRE strongly depend on a via (19), which strongly affects the oceanic and atmospheric patterns and their statistical significance. Interestingly, using $a = 2$ months leads to coherent results between MCA and MRE.

a. Lagged MCA

As in earlier studies, the maximum covariance occurs when Z500 leads SST by 1 month or at lag 0, reflecting the North Atlantic SST anomaly tripole response to NAO forcing (Fig. 8). The covariance and statistical significance decrease at lag 1 (SST leads for positive lag), but the covariance maps remain broadly similar, while a different SST anomaly pattern appears at lag ≥ 2. The resemblance of the mode at lag 1 with that representing the SST response to the atmospheric forcing (also found for the second MCA mode) suggests that it primarily results from atmospheric persistence and the use of monthly data (in the presence of submonthly variability), rather than reflecting a positive feedback between the tripole and the NAO. This would be consistent with Barsugli and Battisti (1998), who showed that the persistence of the lagged covariance between the atmosphere and prior SST is increased by low-frequency SST adjustment to stochastic atmospheric forcing.

In the early winter case, the covariance and statistical significance are small at lag 2 but large at lag 3 and 4 (Fig. 8). As in earlier studies, the mode corresponds to the forcing of a NAO-like signal by the NAH SST anomaly (hereafter the NAH–NAO mode). A comparison with the mode obtained without SST correction, which is based on (A1) rather than (8), shows that the amplitude of the atmospheric response is increased by the SST correction (the corrected SST is smaller but its time series normalized), while the NAH has a stronger center of action off Africa (Fig. 9). This is at odds with Wang et al. (2004), who suggested, based on Granger causality, that the SST anomaly southeast of Newfoundland solely has a significant causal effect on the atmosphere. At larger lag, significance decreases and the (corrected) SST anomaly becomes increasingly deformed, while Z500 increases. Very similar results are obtained in the small SST domain, showing the robustness of the method. Based on lag 3, the Z500 response reaches 45 m east of southern Greenland and half this value over the Azores for a SST anomaly reaching 0.45 K. Introducing the SST correction thus suggests a higher atmospheric sensitivity than estimated by CF02, although it strongly depends on the atmospheric delay (higher sensitivity for a smaller delay, weaker for a larger one). A stronger response is suggested by lag 4, perhaps because of growing bias in the covariance matrices, or because the delay was underestimated. When all the months are considered, the MCA yields nearly the same patterns but with a weaker atmospheric high and reduced significance, as the mode is only 10% significant at lag 4 (Fig. 10). This is consistent with a response primarily taking place in fall and winter.

b. MRE

The most significant results are found when all the months are considered, presumably because the SST covariance matrix in (19) is better conditioned with a larger sample. As the MRE proved rather robust, truncations between TR5 and TR10 were considered. As in the MCA, in most cases a significant mode is found at lag 1, which broadly resembles that at lag 0 showing the SST

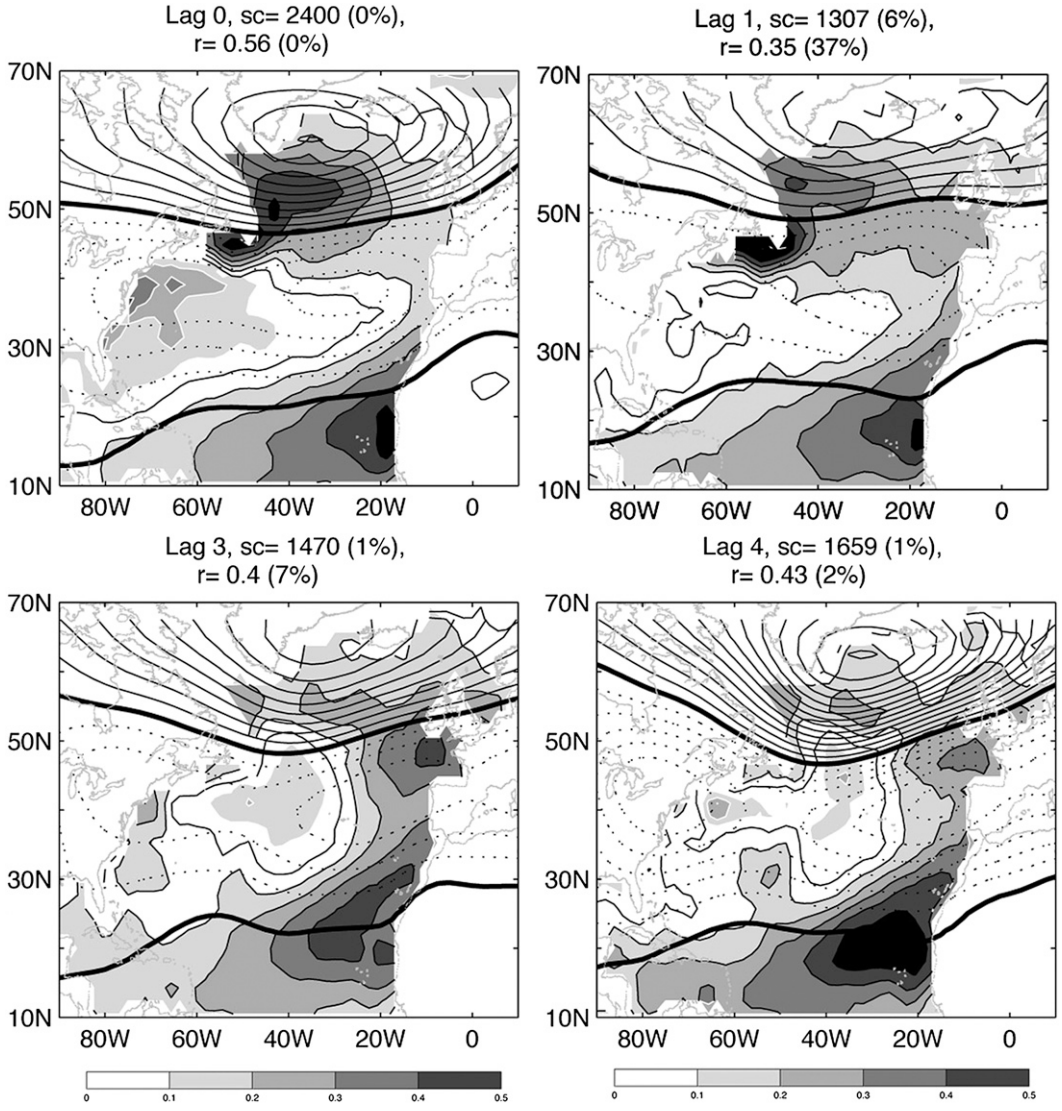

FIG. 8. First MCA mode between SST (K, white contour for negative values) and Z500 in NDJ (contour interval 5 m), assuming a 2-month atmospheric response time: (top) lag (left) 0 and (right) 1; and (bottom) lag (left) 3 and (right) 4. The lag (positive when SST leads) is indicated; sc denotes square covariance and *r* correlation, with the estimated statistical significance. The SST anomaly time series are normalized, so that typical amplitudes are given.

anomaly tripole response to the NAO forcing (not shown). This confirms that lag 1 is indicative of, or strongly biased by, the SST response to the atmosphere. As summarized in Table 1, a significant NAH–NAO mode is found at lag 4 and, occasionally lag 3 or 5, for all truncation between TR6 and TR10. The patterns are stable to truncation and similar in the two SST domains, strikingly resembling the MCA patterns in Fig. 10, except that the maximum SST signal occurs southeast of Newfoundland, in better agreement with Wang et al. (2004), and the negative anomaly of Azores high is stronger (Fig. 11). When Z500 is limited to NDJ, the NAH–NAO mode is also found at lag 3 or 4, albeit only in TR5 to TR7, mostly in the small domain and with slightly less robust patterns (Fig. 12). At lag 3, the amplitudes are comparable to those in the MCA, but the signal is even much larger at lag 4, consistent with the bias high found in unfavorable cases with the artificial data.

Without delay in the atmospheric response, the NAO/SST tripole mode was also found at lag 1, but there was no significant mode at larger lag. This confirms that the atmospheric response should not be considered as instantaneous with monthly averaged data.

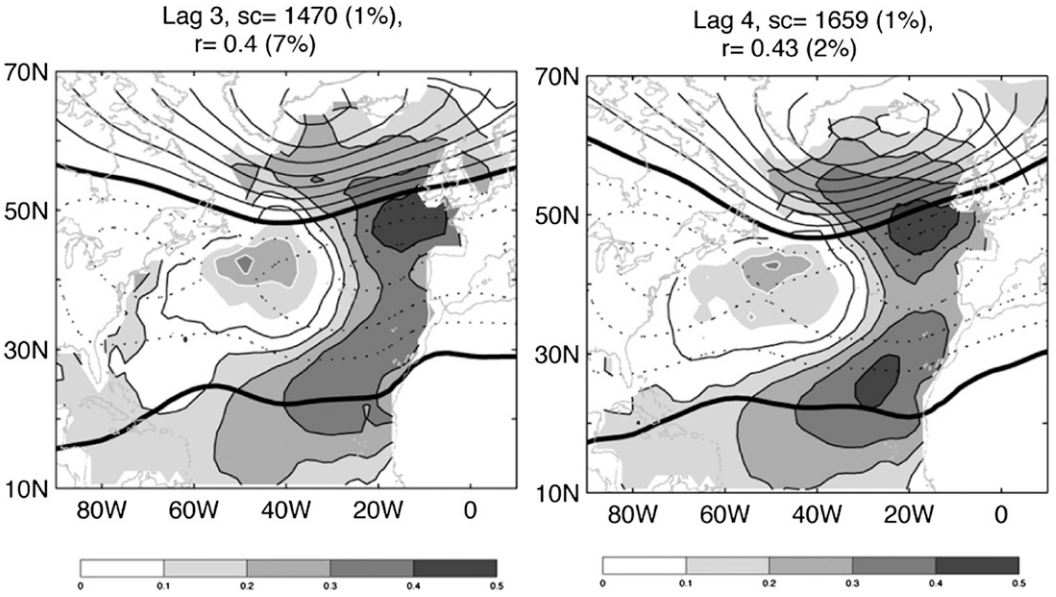

FIG. 9. As in Fig. 8 (bottom panels), but without SST correction.

c. GEFA–SVD

The most significant results with GEFA–SVD are also found when all the months are considered. As they are more sensitive to truncation, we considered truncations between TR3 and TR10. The mode at lag 1 is significant at most truncation between TR5 and TR8, generally resembling that at lag 0 (which should reflect an oceanic response to the atmosphere), while differing somewhat from that at larger lag. This is illustrated in Fig. 13 for TR5, where the mode, a NAO-like Z500 pattern linked to a quadripolar SST pattern, is similar, albeit with a lower statistical significance, to that found in TR5 at lag 1 by LW08 for a different dataset (1957–93). Yet, the mode somewhat differs from that at lag 2 (12% significant, not shown) and lag 3, so that it may not fully represent an oceanic response.

The modes at lag ≥ 2 likely reflect an atmospheric response to SST but, as summarized in Table 2, they proved very sensitive to truncation. For instance, the first mode differs in TR6 and TR7 (Fig. 14, left) from that in TR5, while in TR3, yet another mode is found, resembling the NAH–NAO mode (Fig. 14, right). In addition, the modes are sensitive to domain size at large lag (not shown). In early winter, a significant mode is found at one or two lags between lag 3 and 5 for small truncation (TR3 to TR5), mostly in the small domain, but with very limited SST stability, although all the

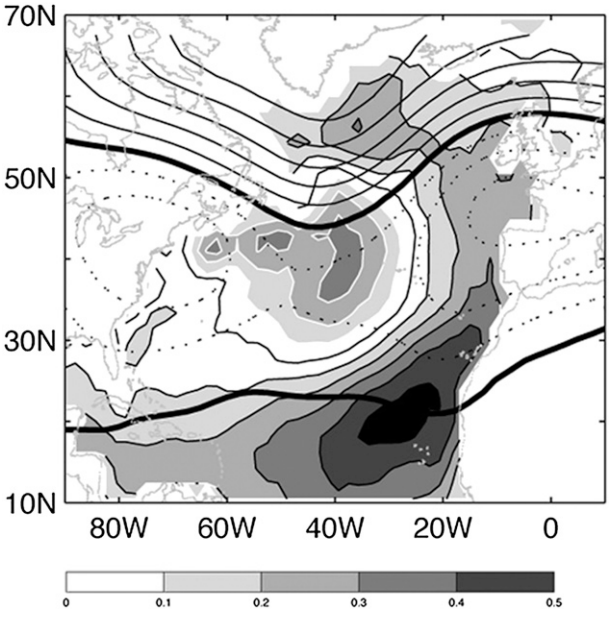

FIG. 10. As in Fig. 8, but based on all months of the year.

TABLE 1. Dependence on lag and truncation of the SST pattern in MRE for the North Atlantic case based on all months of the year. Only modes that are 10% significant in at least one North Atlantic domain are indicated. NAH indicates that the SST pattern resembles the North Atlantic horseshoe. Bold symbols indicate that the mode is significant in the small and the large domains.

MRE	TR5	TR6	TR7	TR8	TR9	TR10
Lag 2						
Lag 3		NAH				
Lag 4		**NAH**	**NAH**	**NAH**	NAH	
Lag 5					**NAH**	NAH

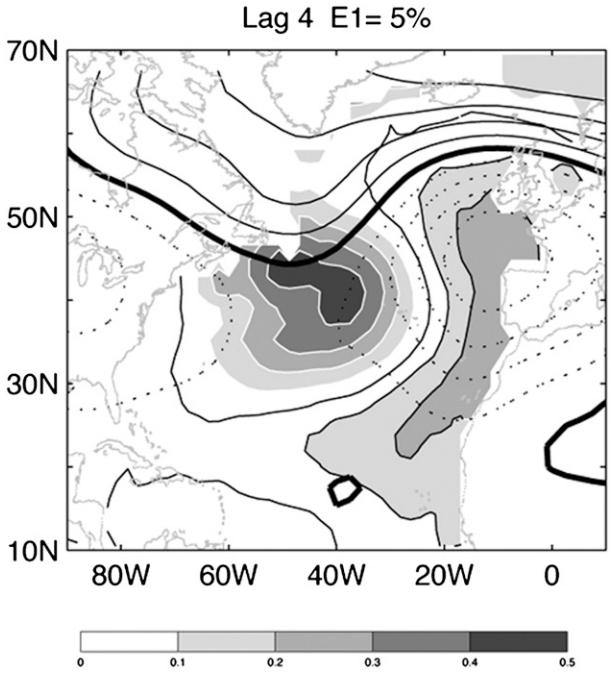

FIG. 11. First MRE mode between SST (K, white contour for negative values) and Z500 (contour interval 5 m) at lag 4 in TR6, assuming a 2-month atmospheric response time. The SST anomaly time series is normalized, so that typical amplitudes are given. The statistical significance is indicated.

atmospheric patterns are NAO-like. In two cases, but not the others, the mode resembles the NAH–NAO mode. Hence, no coherent picture of the optimal SST forcing pattern emerges.

Without delay in the atmospheric response, a mode that broadly resembles that at lag 0 was generally found at lag 1 or 2 (and in a few cases 3), but the patterns lacked robustness and the Z500 amplitude was very large.

5. Summary and conclusions

Three multivariate statistical methods to estimate the influence of SST or boundary forcing on the atmosphere were discussed. Lagged MCA maximizes the lagged covariance between the atmosphere and prior SST. It thus favors large responses and dominant SST patterns, and it is well suited for making predictions. As the MCA does not take into account the possible SST evolution during the time lag, a SST correction was introduced to correctly represent the relation between forcing and response. GEFA–SVD identifies the SST patterns that produce the maximum atmospheric response independently from the SST amplitude; hence it may not detect a large response. A new method, MRE, was designed to estimate the largest boundary-forced atmospheric signal in the sample. In both GEFA–SVD and MRE, the SST covariance matrix must be inverted and SST is considered in a truncated space, thus requiring an appropriate truncation. For climate applications where the emphasis is on detecting or predicting the SST pattern that is responsible for the most atmospheric variance, MRE and MCA are preferable, while GEFA–SVD may be of interest in some theoretical framework. The usefulness of the methods, however, also depends on their biases and robustness, which was investigated.

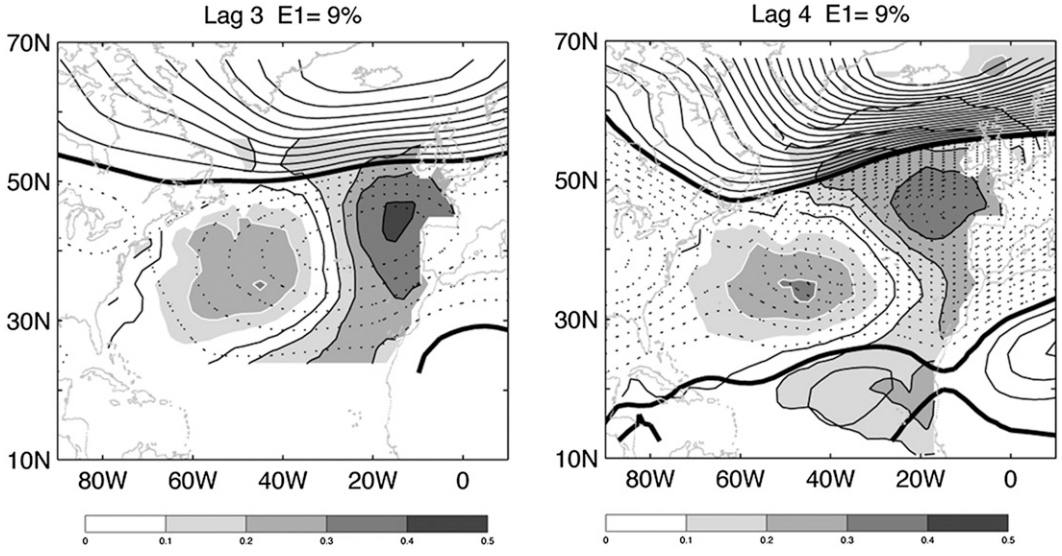

FIG. 12. First MRE mode between SST (K, white contour for negative values) and Z500 in NDJ (contour interval 5 m) in TR6, assuming a 2-month atmospheric response time: lag (left) 3 and (right) 4. The SST anomaly time series are normalized, so that typical amplitudes are given. Lag and statistical significance are indicated.

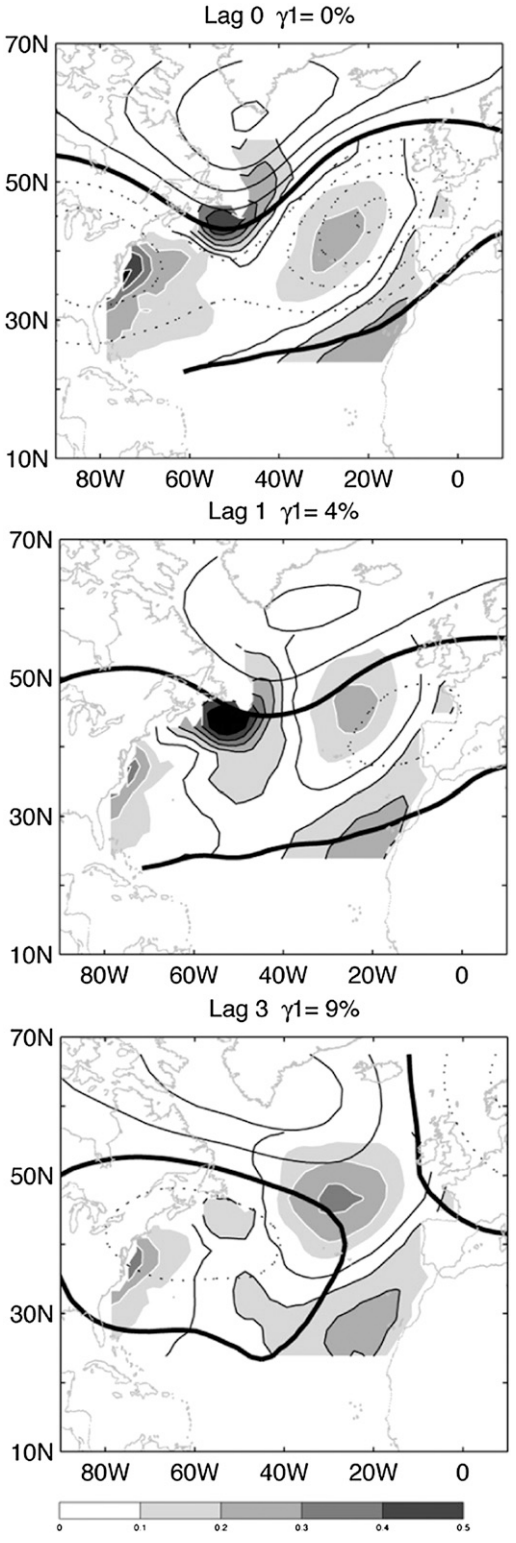

FIG. 13. First GEFA–SVD mode between SST (K, white contour for negative values) and Z500 (contour interval 5 m) in TR5, assuming a 2-month atmospheric response time: (top to bottom) lag 0 to 3. The SST anomaly time series are normalized, so that typical amplitudes are given. Lag and statistical significance are indicated.

The methods were first applied to synthetic data with known properties, following Liu et al. (2008). Four cases were considered, ranging from an idealized case with weak SST advection and spatially uncorrelated atmospheric forcing to the most difficult case with strong advection and correlated forcing. The lagged MCA was very robust and unbiased. However, without correction for the SST evolution, the SST anomaly was a biased version of the SST forcing pattern. The atmospheric patterns in the first two modes were pretty similar to the largest true atmospheric responses, and they were well determined, although in the most unfavorable cases (strong advection) only the first mode could be reliably estimated at small lag. This, however, was also the case for the other methods. Nonetheless, the ensemble mean response remained stable at large lag, when the other methods failed.

The absolute optimal SST pattern for forcing the atmosphere estimated by GEFA–SVD did not have very large amplitude in the synthetic data. Hence, GEFA–SVD led to different modes and weaker atmospheric signals. It was unbiased but sensitive to the EOF truncation and much less robust than MCA, providing reliable estimates only in favorable cases. This reflects its high sensibility to bias and sampling errors in the lagged SST covariance matrix (LW08).

In most cases, MRE provided unbiased estimates of the largest true atmospheric response, and it was nearly as robust as the MCA, with limited sensitivity to the EOF truncation. However, with strong advection, the first mode could only be reliably estimated at shorter lag than with the MCA, and the atmospheric response was biased high. The robustness of the MRE should thus be verified by varying the lag and the truncation. Although both GEFA–SVD and MRE require inverting the SST covariance matrix to estimate the feedback matrix $\mathbf{F}$, MRE proved more robust. Presumably, this occurs because $\mathbf{F}$ is applied to the SST field at each time step to estimate the dominant response, so that the large SST scale smoothes the sampling errors of $\mathbf{F}$.

Applying GEFA to the first SST EOF similarly provided robust estimates of the largest atmospheric response, with little sensitivity on truncation except in very unfavorable cases, consistent with Z. Liu et al. (2011, unpublished manuscript) who showed that the GEFA response to the leading SST EOFs is largely insensitive to the EOF truncation. However, the GEFA response to the second SST EOF was very weak in the large advection case, so that there is no guarantee that GEFA–EOF will always identify large atmospheric signals. Unless there is a-priori evidence that an SST EOF influences the atmosphere, MRE and MCA should be

TABLE 2. Dependence on lag and truncation of the SST pattern in GEFA–SVD for the North Atlantic case based on all months of the year. Only modes that are 10% significant in at least one North Atlantic domain are indicated. The number indicates the number of SST poles in the pattern, except when it resembles the North Atlantic horseshoe pattern, noted NAH. Bold symbols indicate that the same mode is significant in the small and the large domains and two numbers that the SST patterns differ.

GEFA	TR3	TR4	TR5	TR6	TR7	TR8	TR9	TR10
Lag 2				**4**	4			
Lag 3			3	4				
Lag 4	**NAH**			4	3			
Lag 5						3	3, 5	4

favored in climate applications since they determine the SST forcing patterns.

The three methods were applied to observed SST and Z500 monthly anomalies in the North Atlantic during 1958–2008, using all months of the year or, for the atmosphere, NDJ only. Recent modeling (Ferreira and Frankignoul 2005, 2008; Deser et al. 2007) and statistical (Strong et al. 2009) studies suggest that the atmospheric response only reaches its maximum amplitude after about 2 months. This was represented by introducing a delay in the response, assumed to be 2 months. As in CF02 and Frankignoul and Kestenare (2005), and broadly consistent with a delayed response, the MCA gave a highly significant mode when SST leads Z500 in NDJ by 3 and 4 months, reflecting the forcing of the NAO by prior NAH SST anomalies. This NAH–NAO mode was also seen with all months of the year but with less significance. The SST correction, which does not affect statistical significance or the atmospheric pattern, increased the estimated atmospheric sensitivity and slightly changed the SST forcing pattern.

Because MRE and GEFA–SVD are more sensitive to sampling errors, the most significant results were obtained with all months of the year. MRE gave the NAH–NAO mode as in the MCA, although the maximum SST occurred southeast of Newfoundland rather than off Africa, consistent with Wang et al. (2004). The mode was robust to domain size and EOF truncation. Since MRE was shown with the artificial data to provide the best estimate of the largest true response, the resemblance with the MCA mode confirms that MCA is well adapted to detecting large signals. MRE seems more powerful than MCA when the sample is large but less when the sample is small since the mode was not as stable in early winter and more sensitive to truncation.

GEFA–SVD proved sensitive to lag and truncation and should be used with caution. The NAH–NAO mode was found with a very strong EOF truncation but not otherwise, suggesting that the atmosphere might be more sensitive to other, more complex SST patterns of smaller magnitude. However, the patterns were not robust and no coherent picture of the optimal SST forcing pattern emerged, presumably because GEFA–SVD would require a much larger sample to provide robust results.

The three methods gave a significant mode when Z500 follows SST by 1 month. However, it broadly resembled the mode found when SST lags the atmosphere, which reflects the SST response to atmospheric forcing. This resemblance suggests that the mode at lag 1 primarily reflects, or is strongly influenced by, an oceanic response,

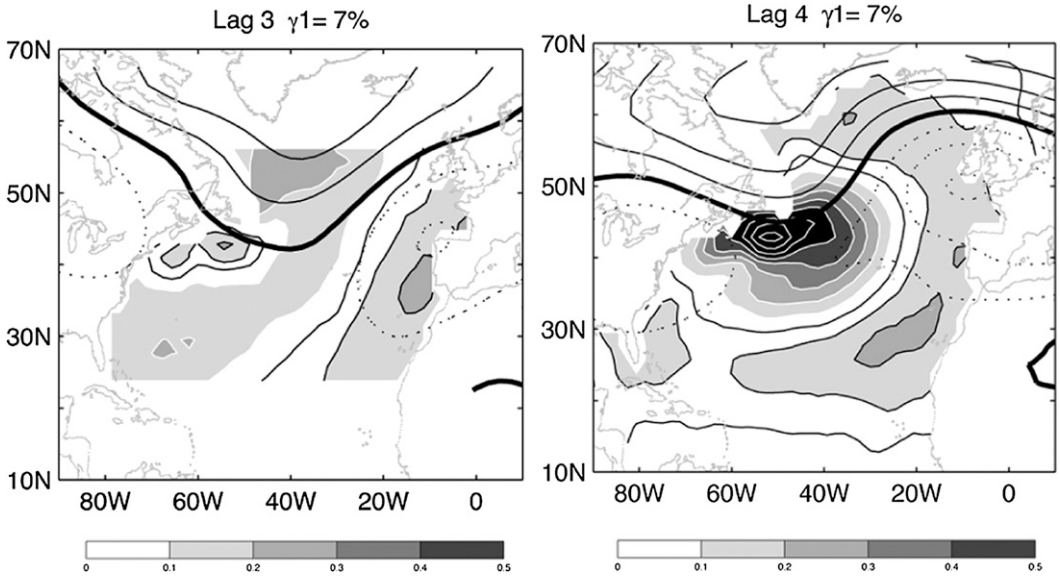

FIG. 14. As in Fig. 13, but for (left) lag 3 in TR6 and (right) lag 4 in TR3.

consistent with the reduced thermal damping of Barsugli and Battisti (1998).

In summary, we recommend MRE and MCA for finding large boundary-forced signals, although large lags should be avoided as they overestimate the atmospheric response in realistic settings. MRE provides the best estimate of the largest atmospheric response if the sampling is sufficiently large, but it is more sensitive than MCA to the assumed delay in the atmospheric response. We stress that MRE only detected a significant SST influence when introducing the delay and the 2-month delay lead to consistent results between MCA and MRE. However, the estimated atmospheric sensitivity increased with the lag, which suggests that the delay may have been underestimated. A better representation of the transient atmospheric response to boundary forcing should be implemented in future studies.

Acknowledgments. This work was initiated while Z. Liu was an invited professor at the Université Pierre et Marie Curie. We thank N. Sennéchael for her help and the reviewers for their thoughtful and constructive comments. Support (to CF) from the Institut Universitaire de France is acknowledged.

APPENDIX

Lagged MCA

Using (7), the homogeneous covariance map of $\mathbf{T}$ and the heterogeneous covariance map of $\mathbf{X}$ are given for mode k respectively by

$$\frac{1}{L}\sum \mathbf{T}(t-\tau)b_k(t-\tau) = \mathbf{C_{TT}}(0)\mathbf{v}_k \quad \text{and} \tag{A1}$$

$$\frac{1}{L}\sum \mathbf{X}(t)b_k(t-\tau) = \mathbf{C_{XT}}(\tau)\mathbf{v}_k = \mathbf{UDV}^{\mathrm{T}}\mathbf{v}_k = \mathbf{u}_k\sigma_k. \tag{A2}$$

Scaled maps representing the amplitude of the $\mathbf{T}$ and $\mathbf{X}$ anomalies associated with one standard deviation of $b_j(t-\tau)$ are obtained by dividing (A1) and (A2) by the standard deviation s_{bk} of $b_k(t-\tau)$.

A dimensional version of the corrected SST pattern (8) is obtained by projecting the $\mathbf{T}$ field onto the (nonorthogonal) set $\tilde{\mathbf{q}}_k = \mathbf{q}_k|\mathbf{q}_k|^{-1}$

$$\mathbf{T}(t) = \sum_1^K \tilde{\mathbf{q}}_k d_k(t) \tag{A3}$$

and calculating the standard deviation s_{dk} of $d_k(t)$. Relation (8) becomes

$$\frac{\sigma_k}{|\mathbf{q}_k|}s_{\mathrm{dk}}\mathbf{u}_k = \mathbf{F}s_{\mathrm{dk}}\tilde{\mathbf{q}}_k. \tag{A4}$$

REFERENCES

Barsugli, J. J., and D. S. Battisti, 1998: The basic effects of atmosphere–ocean thermal coupling on midlatitude variability. *J. Atmos. Sci.,* **55,** 477–493.

Bretherton, C. S., C. Smith, and J. M. Wallace, 1992: An intercomparison of methods for finding coupled patterns in climate data. *J. Climate,* **5,** 541–560.

Czaja, A., and C. Frankignoul, 1999: Influence of the North Atlantic SST on the atmospheric circulation. *Geophys. Res. Lett.,* **26,** 2969–2972.

——, and ——, 2002: Observed impact of North Atlantic SST anomalies on the North Atlantic Oscillation. *J. Climate,* **15,** 606–623.

Deser, C., R. Thomas, and S. Peng, 2007: The transient atmospheric circulation response to North Atlantic SST and sea ice anomalies. *J. Climate,* **20,** 4751–4767.

Feldstein, S. B., 2000: The timescale, power spectra, and climate noise properties of teleconnection patterns. *J. Climate,* **13,** 4430–4440.

Ferreira, D., and C. Frankignoul, 2005: The transient atmospheric response to midlatitude SST anomalies. *J. Climate,* **18,** 1049–1067.

——, and ——, 2008: Transient atmospheric response to interactive SST anomalies. *J. Climate,* **21,** 576–583.

Frankignoul, C., and K. Hasselmann, 1977: Stochastic climate models. II: Application to sea-surface temperature variability and thermocline variability. *Tellus,* **29,** 284–305.

——, and E. Kestenare, 2002: The surface heat flux feedback. Part I: Estimates from observations in the Atlantic and the North Pacific. *Climate Dyn.,* **19,** 633–647.

——, and ——, 2005: Observed Atlantic SST anomaly impact on the NAO: An update. *J. Climate,* **18,** 4089–4094.

——, and N. Sennéchael, 2007: Observed influence of North Pacific SST anomalies on the atmospheric circulation. *J. Climate,* **20,** 592–606.

——, A. Czaja, and B. L'Heveder, 1998: Air–sea feedback in the North Atlantic and surface boundary conditions for ocean models. *J. Climate,* **11,** 2310–2324.

Friederichs, P., and A. Hense, 2003: Statistical inference in canonical correlation analysis exemplified by the influence of North Atlantic SST on European climate. *J. Climate,* **16,** 522–534.

Kistler, R., and Coauthors, 2001: The NCEP–NCAR 50-Year Reanalysis: Monthly means CD-ROM and documentation. *Bull. Amer. Meteor. Soc.,* **82,** 247–267.

Liu, Q., N. Wen, and Z. Liu, 2006: An observational study of the impact of the North Pacific SST on the atmosphere. *Geophys. Res. Lett.,* **33,** L18611, doi:10.1029/2006GL026082.

Liu, Z., and L. Wu, 2004: Atmospheric response to North Pacific SST: The role of ocean–atmosphere coupling. *J. Climate,* **17,** 1859–1882.

——, and N. Wen, 2008: On the assessment of nonlocal climate feedback. Part II: EFA-SVD analysis and optimal feedback. *J. Climate,* **21,** 5402–5416.

——, M. Notaro, J. Kutzbach, and N. Liu, 2006: Assessing global vegetation–climate feedbacks from the observation. *J. Climate,* **19,** 787–814.

——, Y. Liu, L. Wu, and R. Jacob, 2007: Seasonal and long-term atmospheric responses to reemerging North Pacific Ocean

variability: A combined dynamical and statistical assessment. *J. Climate,* **20,** 955–980.

——, N. Wen, and Y. Liu, 2008: On the assessment of nonlocal climate feedback. Part I: The generalized equilibrium feedback assessment. *J. Climate,* **21,** 134–148.

Park, S., C. Deser, and M. A. Alexander, 2005: Estimation of the surface heat flux response to sea surface temperature anomalies over the global oceans. *J. Climate,* **18,** 4582–4599.

Rodwell, M. J., and C. K. Folland, 2002: Atlantic air–sea interaction and seasonal predictability. *Quart. J. Roy. Meteor. Soc.,* **128,** 1413–1443.

Strong, C., G. Magnusdottir, and H. Stern, 2009: Observed feedback between winter sea ice and the North Atlantic Oscillation. *J. Climate,* **22,** 6021–6032.

von Storch, H., and F. W. Zwiers, 1999: *Statistical Analysis in Climate Research*. Cambridge University Press, 342 pp.

Wang, W., B. T. Anderson, R. K. Kaufmann, and R. B. Myneni, 2004: The relation between the North Atlantic Oscillation and SSTs in the North Atlantic basin. *J. Climate,* **17,** 4752–4759.

Wen, N., Z. Liu, Q. Liu, and C. Frankignoul, 2010: Observed atmospheric responses to global SST variability modes: A unified assessment using GEFA. *J. Climate,* **23,** 1739–1759.